

Influence of Annealing Condition on Structural Properties of Nano Crystalline $Fe_{73.5}Ag_1Nb_3Si_{13.5}B_9$ Alloy

A. K. M. Asaduzzaman^{1*}, Md. Abdul Gofur², M. A. Gafur³ and S. S. Sikder⁴,

¹Department of Physics Military Collegiate School Khulna (MCSK), Khulna, Bangladesh

²Department of Physics Dr. AbdurRazzak Municipal College Jashore, Bangladesh,

³Bangladesh Council of Scientific and Industrial Research (BCSIR), Dhanmondi, Dhaka-1205,

⁴Department of Physics, Khulna University of Engineering & Technology, Khulna-9203, Bangladesh.

*Corresponding Author: A. K. M. Asaduzzaman

Abstract

The kinetics of crystallization of different crystalline phases of $Fe_{73.5}Ag_1Nb_3Si_{13.5}B_9$ has been studied by differential thermal analysis (DTA). DTA diagrams of amorphous ribbons were taken in nitrogen atmosphere with continuous heating rate of 10 -50°C/min in step of 10°C. The primary exothermic peaks temperature for α -Fe (Si) was found 603⁰C and the secondary exothermic peak temperature for Fe_2B phase was found 768⁰C at the same heating rate 20⁰C/min. The kinetics of glass formation and crystallization in composition is studied as affected to differential thermal analysis. Thermal analysis experiment and from the obtained data the activation energy is found 4.37eV and 4.45eV respectively. For primary crystallization product, α -Fe(Si) phase of the ribbon and nanocrystalline state was evaluated by XRD. The alloy has been annealed in a controlled way in the temperature range of 450⁰ C to 800⁰C for 30 minutes. By XRD experiment crystallization onset temperature for α -Fe(Si) phase was found around 650⁰C. The lattice parameter, the Si content in bcc nanograins and the grain size of bcc grains can easily be calculated from the fundamental peaks of (110) reflection. In the optimized annealing condition the grain size has been obtained in the range 9-30 nm. The lattice parameter and Si at % shows an inverse relationship indicating that silicon diffuses out of α -Fe(Si) grain for which the size α -Fe(Si) lattice is regained. The curie temperature was found 653⁰K.

Keywords: DTA, XRD, VSM, Activation energy, Lattice Parameter and Curie Temperature.

Date of Submission: 01-08-2020

Date of Acceptance: 16-08-2020

I. Introduction

The nanocrystalline structures which substantially improve the magnetic properties of Fe-Cu-Nb-Si-B or Fe-Zr-B types alloys is presently attracting much interest [1-2]. In this structures the particle diameter is less than 20 nm and the crystallization from the amorphous phase produces the fine structure of a bcc iron based solid solution. Amorphous alloys provide an extremely convenient-precursor material for preparation of nanocrystals through the crystallization process controlled by thermal treatments [3-8]. In 1988 Yoshizawa, Oguma and Yamauchi at Hitachi metals Ltd developed the first nanocrystalline ultra soft magnetic alloy called FINEMET having composition $Fe_{73.5}Nb_3Cu_1Si_{13.5}B_9$ from the Fe-Si-B amorphous alloys to which addition of Cu and Nb were added [9]. The Cu and Nb additives play a key role in the formation of the nanocrystalline state Cu by multiplying the nucleation centres and Nb by inhibition the grain growth [10]. The annealing parameters (time, temperature and atmosphere) must be controlled and the nanocrystalline state can be obtained after conventional annealing under vacuum or atmosphere for typically 1h at >550⁰C. The FINEMET consists of a two phase microstructure in its optimally annealed condition. The microstructure is made up of a ferromagnetic bcc α -Fe (Si) phase and /or Do_3 type of ordered Fe (Si) phase with grain size of 10-15nm embedded in this residual ferromagnetic amorphous matrix of about 1-2nm thickness. These represent a new family of excellent soft magnetic core materials and have stimulated an enormous research activity due to their potential applications [11-12]. Müller *et. al.* [13] studied the influence of Cu/Nb content and annealing condition on the microstructure and the magnetic properties of FINEMET alloys. Grain size, phase composition and transition temperature were observed to depend on the Cu/Nb content. This paper focuses on the experimental investigation of crystallization behaviour, nanocrystalline structure formation and magnetic properties of $Fe_{73.5}Ag_1Nb_3Si_{13.5}B_9$ alloys in the amorphous and annealed states.

II. Materials And Methods

Amorphous ribbons with the nominal composition $Fe_{73.5}X_1Nb_3Si_{13.5}B_9$ [X = Cu, Ag & Au] were prepared in an arc furnace on a water-cooled copper hearth under an atmosphere of pure Ar. Their purity and origin of the constituent elements were Fe (99.9%), Ag (99.9%), Au (99.9%), Nb(99.9%), Cu (99.9%), Si (99.9%) and B (99.9%) as obtained from Johnson Mathey (Alfa Aesar Inc.). Before melting, the furnace chamber was evacuated (10^{-4} torr), and flashed with Ar gas. The process was repeated several times to get rid of residual air and finally the furnace chamber were kept in an Ar atmosphere. The mother alloys, which are formed in the form of buttons in a furnace by sudden cooling and then cut into small pieces and is introduced in the quartz tube.

Melt spinning is a widely used production method for rapidly solidifying materials as well as preparing amorphous metallic ribbon [14-15]. In order to prepare amorphous of $Fe_{73.5}Ag_1Nb_3Si_{13.5}B_9$ alloys, the melt spinning facilities was used at the Centre for Materials Science, National University of Hanoi, Vietnam. The resulting ribbon samples had thickness of about 20-25 μm and width ~ 6 mm. The Factors that is used to Control the thickness of ribbons when angular velocity $\omega = 2000$ rev/min and Surface velocity $V = 20$ m/s to 30 m/s. Gap between nozzle and rotating copper drum (h) = 200 to 30 μm . Oscillations of the rotating copper drum both static and dynamic has maximum displacement 1.5 to 5 μm . Pressure = 0.2 to 3.0 bar at argon atmosphere. Temperature of molten metals $T_m \approx 1500^\circ C$; the temperature did not exceed $1800^\circ C$ otherwise quartz tube would be melted. A steady flow of the molten metals on the surface of the rotating drum needs to be ensured. The activation energy was calculated From Kissinger's equation $E = -kT_p \ln \frac{\beta}{T_x^2}$, here E is the activation energy, β is heating rate and the respective crystallization temperature (T_x^2). From the obtained data of XRD the lattice parameter has been calculated using equation, $2d \sin \theta = \lambda$ and, $a_0 = d\sqrt{2}$, where $\lambda = 1.54178 \text{ \AA}$ for $Cu - K_\alpha$ radiation and a_0 is the determined lattice parameter within an error estimated to be $\pm 0.0001 \text{ \AA}$.

Grain size is determined using the following formula, $D_g = \frac{0.9\lambda}{\beta \cos \theta}$, β = FWHM (full width at half maximum) of the peak in radian

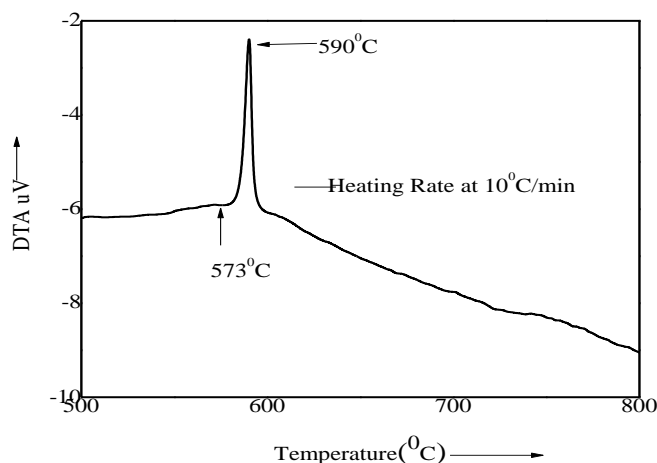


Figure 1(a)

Si-contents for the nanograins develop during the isothermal annealing at various temperatures have been calculated using the equation is $X = \frac{(a_0 - 2.8812)}{0.0022}$ Where X is at. % Si in the nanograins. Temperature dependent magnetization were performed by VSM.

III. Result And Discussion

Differential Thermal Analysis(DTA):

DTA traces of as-cast nanocrystalline amorphous ribbon $Fe_{73.5}Ag_1Nb_3Si_{13.5}B_9$ alloy taken in the Nitrogen atmosphere with the heating rates of $10^{\circ}C - 50^{\circ}C$ /minute at the step of $10^{\circ}C$ with continuous heating from room temperature to $800^{\circ}C$, are presented in figure 1(a) to figure 1(e) respectively. Two well defined exothermic peaks typical for two steps of crystallization processes are manifested from the DTA traces. The first one corresponds to the crystallization of α -Fe(Si) phase and the second one is related to the crystallization of Fe_2B . The onset of crystallization temperatures T_{x_1} and T_{x_2} have been estimated from DTA traces.

From figure 1.(f) represents a combination of all DTA traces of amorphous ribbon alloy and it is observed that the crystallization of each phase has occurred over a wide range temperature and that the peak temperatures shifted to higher values with the increase of heating rate. That means it requires more that energy for the formation of crystalline phases with increasing heating rates. Table1 crystallization peak temperatures of two phases (T_{p_1} and T_{p_2}) and crystallization starting temperatures of two phases (T_{x_1} and T_{x_2}) are given for different heating rates.

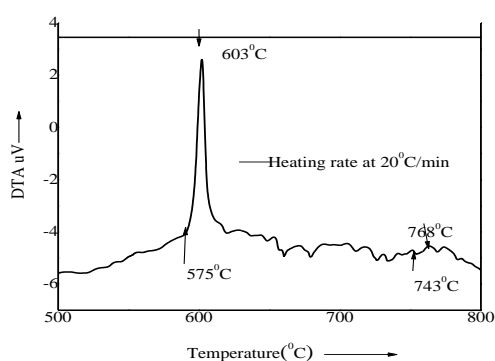


Figure 1(b)

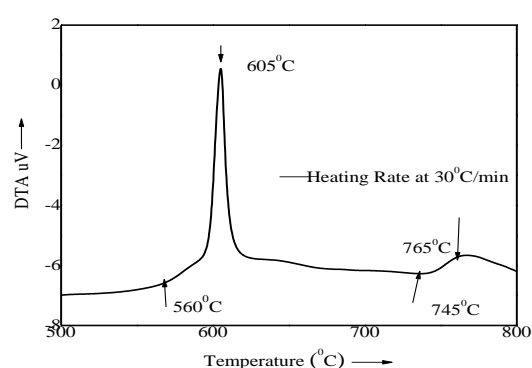


Figure 1(c)

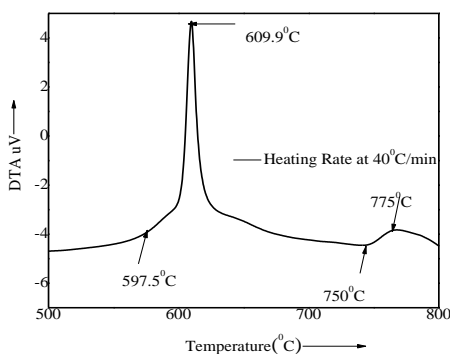


Figure 1(d)

Figure 1. DTA trace of as cast amorphous ribbon $Fe_{73.5}Ag_1Nb_3Si_{13.5}B_9$ at the heating rate of (a) $10^{\circ}C$ /min (b) $20^{\circ}C$ /min(c) $30^{\circ}C$ /min(d) $40^{\circ}C$ /min(e) $50^{\circ}C$ /min

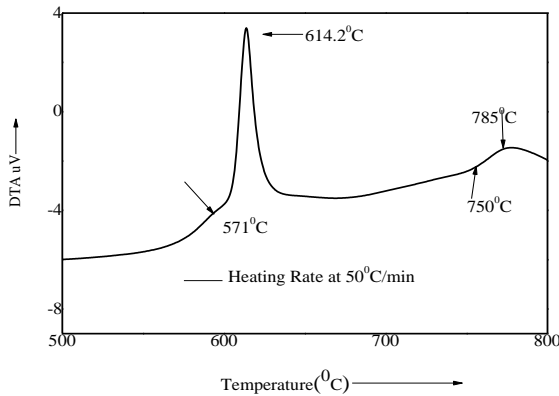


Figure 1(e)

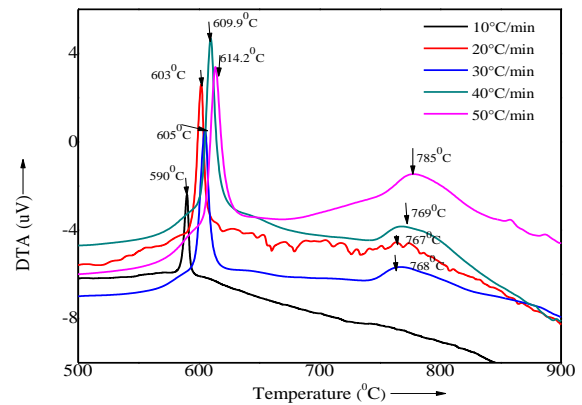


Figure 1(f) Effects of heating rate on DTA traces of nanocrystalline amorphous ribbon with composition $Fe_{73.5}Ag_1Nb_3Si_{13.5}B_9$ at the heating rate of $10^{\circ}C$ to $50^{\circ}C$ /min.

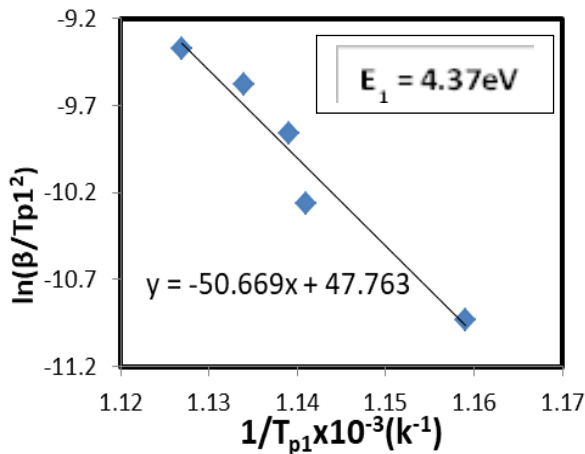


Figure 2(a)

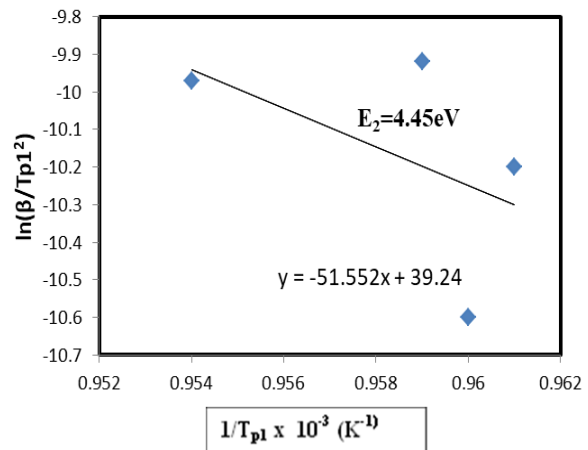


Figure 2(b)

Figure 2. Kissinger's plot to determine the activation energy of α -Fe(Si) phase for $Fe_{73.5}Ag_1Nb_3Si_{13.5}B_9$ alloy (a) before annealing (b) after annealing.

It has been observed that the crystallization temperature range of first phase occurred within $12.4^{\circ}C$ to $45^{\circ}C$. But this range for second crystallization phase is $19^{\circ}C$ to $35^{\circ}C$. So it is notable that the crystallization temperature range for first peak is always larger than the second peak but except heating rate $40^{\circ}C$ /minute; i.e. is experimental error. It is also observed that the peak temperature shifts to higher values and the crystallization temperature range increases with the increase of heating rates. The activation energy of T_{x1} [α -Fe (Si)] and T_{x2} [Fe_2B] phases have been calculated from Kissinger's plot shown in figure 2. It shows that first thermal crystallization activation energy of α -Fe(Si) phase E_1 is 4.37 eV and second Fe_2B phase E_2 is 4.45 eV.

Table 1. The values of crystallization onset temperature, peak temperature with respect to heating rate and activation energy of the nanocrystalline amorphous ribbon with composition $Fe_{73.5}Ag_1Nb_3Si_{13.5}B_9$

Heating rate $\beta^{\circ}C/min$	Onset temperature $T_{x1}^{\circ}C$	1 st temperature $T_{p1}^{\circ}C$	Peak Temperature range of 1 st state in $^{\circ}C$	Activation energy of the peak before annealing (eV)	Activation energy of the peak after annealing (eV)
10	573	590	17	4.37	4.45
20	575	603	28		
30	560	605	45		
40	597.5	609.9	12.4		

X-ray diffraction analysis(XRD)

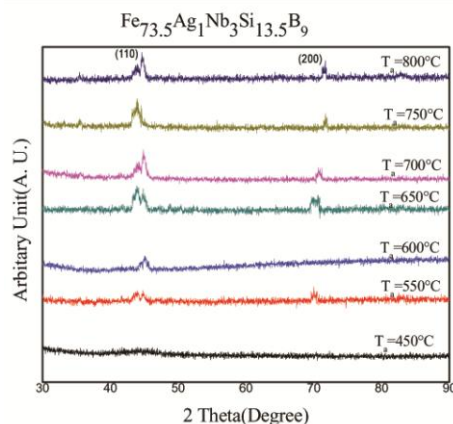


Figure3. XRD spectra of Fe_{73.5}Ag₁Nb₃Si_{13.5}B₉ alloys of annealed at different temperatures at constant annealing time 30 minutes

In the present work, structure of the Fe_{73.5}Ag₁Nb₃Si_{13.5}B₉ alloys, annealed at temperature 450°C to 800°C, are investigated by the XRD. From XRD patterns 450°C to 600°C indicates the amorphous nature. Due to annealing at 650°C, the first crystallization peak was found at the angle 45°. It means at the annealing temperature below 650°C no crystalline peak has been detected. After heat treatment at T_a = 650°C initiation of crystallization takes place. For annealing at higher temperature i.e. 650°C, 700°C, 750°C and 800°C, the α-Fe(Si) phase were found at the lower values of 2θ at 45°, 44.84°, 44.852°, 44.88° and 44.66° respectively with 100% peak intensity on (110) line. All the results of θ, d-value, FWHM, a₀, D_g and at.% Si at different annealing temperature of these composition are listed in Table 2.

Figure 4 shows that, with increase in annealing temperature lattice parameter increase. Observed lattice parameter at various annealing temperature for the present alloy are significantly less than that of pure Fe is 2.8664Å. It is also observed that the Si-content in α-Fe(Si) phase decrease with annealing temperature up to 800°C and figure represents the inverse relationship between lattice parameter and silicon content.

From figure 5 represents that grain size (D_g) constant up to 700°C and above this annealed temperature grain size increases. In the range of annealing temperature 650°C to 800°C, the grain size remains in the range of 9 to 30nm. Grain growth rapidly and attain value 20nm at 750°C indicating formation of boride phase. Grain size increases with annealing temperature from a value of D_g = 30nm for T_a = 800°C while Si content rapidly decreases with T_a. This is contradictory to original FINEMET alloy. This may be resulted due to higher physical distortion and internal strain. These facts reveal that heat treatment temperature should be limited with in 650°C to 700°C to obtain optimum soft magnetic behavior, which will be clear that constant grain size.

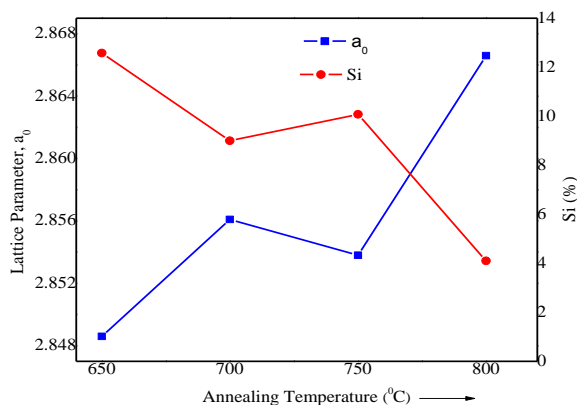


Figure 4. Change of Si (at. %) content and Lattice Parameter with different annealing temperature for the sample with composition Fe_{73.5}Ag₁Nb₃Si_{13.5}B₉

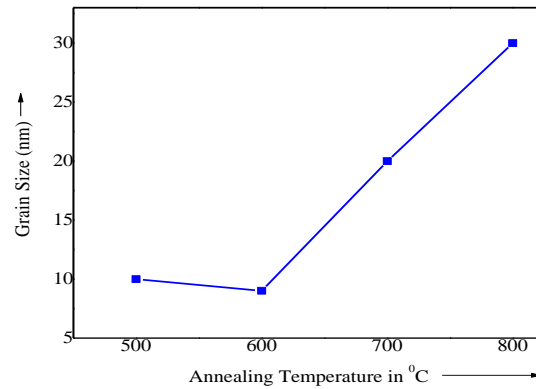


Figure 5. Change of Grain Size with different annealing temperature for the sample with composition $Fe_{73.5}Ag_1Nb_3Si_{13.5}B_9$

Table 2. Experimental XRD data of nanocrystalline $Fe_{73.5}Ag_1Nb_3Si_{13.5}B_9$ amorphous ribbon at different annealing temperatures

Annealing Temp. in °C	Temp.	θ (deg.)	d (Å)	FWHM (deg.)	a_0 (Å)	D_g (nm)	Si (at. %)
450	--	--	--	--	--	--	--
550	--	--	--	--	--	--	--
600	--	--	--	--	--	--	--
650	22.50	2.013	0.82	2.8468	10	12.58	
700	22.42	2.0196	0.87	2.8561	9	9.00	
750	22.44	2.018	0.42	2.8538	20	10.00	
800	22.33	2.027	0.28	2.8666	30	4.1	

Temperature Dependence of specific Magnetization:

The variation of saturation magnetization (M_s) as a function of temperature in the range 300 k to 800 k measured with an applied field of 10kOe in the amorphous state for the nanocrystalline amorphous samples with composition $Fe_{73.5}Ag_1Nb_3Si_{13.5}B_9$ are shown in figure 7.

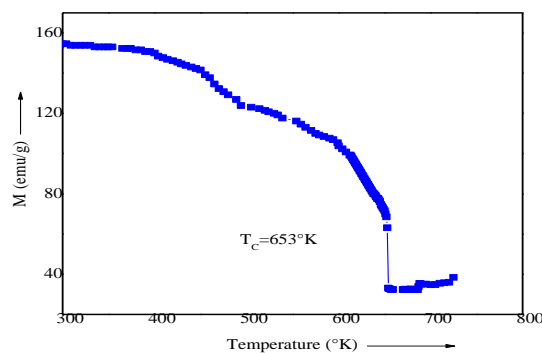


Figure 7 (a) Temperature dependence of specific magnetization of amorphous nanocrystalline ribbons with composition $Fe_{73.5}Ag_1Nb_3Si_{13.5}B_9$ alloy

From these curve T_c has been determined as the temperature corresponding to the inflexion point where the rate change of magnetization with respect to temperature is maximum shown in figure 7(a), 7(b) .As the temperature approaches to the T_c , magnetization falls more rapidly near to zero as the thermal energy exceeds the magnetic ordering or the exchange energy.

The accurate determination of T_c of amorphous material is really difficult due to irreversible components of the structural relaxation like long range internal stress, topological and chemical short range order.

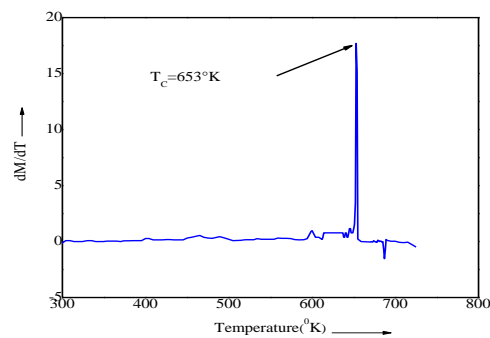


Figure 7(b) $\frac{dM}{dT}$ versus temperature curve of amorphous Nanocrystalline ribbons with composition $Fe_{73.5}Ag_1Nb_3Si_{13.5}B_9$ alloy.

IV. Conclusions

The crystallization behavior of the sample was investigated by the experiments of DTA and XRD and VSM as a result the following outlined can be concluded:

- DTA experiment was performed for five different rates 10 to 50°C/min in steps of 10⁰C/min up to a temperature of 800°C. DTA reveals the primary and secondary crystallization onset temperature with the manifestation of two well defined exothermic peaks corresponding to nanocrystallization α -Fe(Si) (T_{x_1}) and Fe₂B(T_{x_2}) phases respectively. First crystallization phase T_{x_1} indicates stability of amorphous state of structural stability and magnetic ordering values of T_{x_1} are observed 575°C for $Fe_{73.5}Ag_1Nb_3Si_{13.5}B_9$ with heating rate 20°C/min.
- The activation energy of the first crystallization phase α -Fe(Si) and second crystallization phase Fe₂B phase before and after annealing is found 4.37eV and 4.45eV respectively.
- The amorphous stage of the as-cast ribbon has been confirmed by XRD. The evolution of the primary phase on annealed samples has been confirmed as α -Fe(Si) phase with average grain grown in the amorphous matrix 9 - 30 nm for $Fe_{73.5}Ag_1Nb_3Si_{13.5}B_9$. This is quite reasonable since their crystallization onset temperature is 650°C and higher. The lattice parameter and Si at% shows an inverse relationship indicating that Si diffuses out of α -Fe(Si) grain for which the size of α -Fe lattice is regained.
- The curie temperature of the sample has been determined by temperature dependence saturation magnetization that is 380°C. The sharp fall of M_s at T_c indicates that the material is quite homogeneous.

Finally, concluded that promising initial results on FINEMET alloy suggest Cu replace Ag that that might also find their way in high temperature soft magnetic applications. The playground of microstructural engineering of soft magnetic properties will undoubtedly after new discoveries for future materials scientist and engineers.

Acknowledgement

We are grateful to Bangladesh Council for Scientific and Industrial Research(BCSIR) for giving experimental facilities and cordial co-operations.

Reference

- [1]. Mohammad Mahmuduzzaman Tawhid, Sujit Kumar Shil, Mohammad Tahmid Shihab, Shibendra Shekher Sikder, Mohammad Abdul Gofur, "The Crystallization Kinetics, Structural and Magnetic Properties of Amorphous Ribbon as Affected by Annealing" ; American Journal of nanoresearch and Application. Vol6, No.3, pp.60-66, 2018.
- [2]. Kazi Haniun Maria, Mondal S. P, Shamima Chowdhury, Sikder S. S, Hakim M. A. and Saha D. K; "Effect of annealing temperature on the soft magnetic properties of $Fe_{73.5}Cu_1Nb_1Si_{13.5}B_9$ Amorphous alloys", Journal Emerging Trends sciences (JETEAS), 2 (i), 102 - 108, 2011
- [3]. Kulik T., Hernando A. and Vasquez M.; "Correlation between structure and the magnetic properties of amorphous and nanocrystalline $Fe_{73.5}Cu_1Nb_3Si_{22.5-x}B_9$ [X = Cu, Ag & Au] alloys", J. Magn. Magn. Mater., 133, 310, 1994.
- [4]. Jing Zhi, Kai-Yuan He, Li-Zhi Cheng and Yu-Jan Fu; "Influence of the elements Si/B on the structure and magnetic properties of nanocrystalline $(Fe,Cu,Nb)_{73.5}Si_xB_{22-x}$ [X = Cu, Ag & Au] alloys"; J. Magn. Magn. Matter 9, 153 315, 1996.
- [5]. Kane S. N, Sarabhai S., Gupta A., Varga L. K, Kulit T.; "Effect of quenching rate on crystallization in $Fe_{73.5}Cu_1Nb_3Si_{22.5-x}B_9$ alloys"; J. Magn. Magn. Mater., 215-216, 372, 2000.
- [6]. Bigot J., Lecaude N., Perron J. C., Millan C., Ramiarinjoana C. and Rialland J. F., "Influence of annealing condition on nanocrystallization and magnetic properties in $Fe_{73.5}Cu_1Nb_3Si_{22.5-x}B_9$ [X = Cu, Ag & Au] alloy", J. Magn. Magn. Matter., 133, 29, 1994.

- [7]. Hasiak M., Zbrozyczk J., Olszewki J., Ciuzynska W. H., Wyslocki B., Blachowicz A., "Effect of cooling rate on magnetic properties of amorphous and nanocrystalline alloys"; 215-216, 410, 2000.
- [8]. Saroat Noor, Sikder S. S., Saha D. K. and Hakim M. A., "Time and temperature dependence of nanocrystalline and initial permeability of FINEMET alloy"; Nuclear science and application, No.15, 13-19, June 2006.
- [9]. Yoshizawa Y., Osuma S., Yamauchi K.; "New Fe-based soft magnetic alloys composed of ultra-fine grain structure", J. Appl. Phys., 6044 – 6046, 1998.
- [10]. Jing Zhi, Kai-Yuan He, Li-ZbiChing and Yu - Jan Fu; "Influence of the elements Si/B on the structure and magnetic properties of nanocrystalline (Fe, Cu, Nb)_{77.5}Si_xB_{22.5-x} Alloys". J. Magn, Magn. Mater, 153, 315, 1996.
- [11]. Saroat Noor; M Phil Thesis, Department of Physics, KUET, Khulna, March 2005
- [12]. Saha D. K. and Hakim M. A.; "Crystallization behavior of amorphous nanocrystalline soft magnetic alloys", Bangladesh Academy of Science, Vol. No.2, pp.177-187, 2006.
- [13]. Hakim M. A., Sikder S. S., Sultan Mahmud Md. and ManjuraHaque S.; Dilution of magnetic moment of Fe by Cr for Fe_{73.5-x}Cu₁Cr_xNb₃Si_{13.5}B₉ and field cooled and zero field cooled behavior for higher Cr-content"; Journal of Korean Physical Society (JKPS), Vol.52, No.5, 2008
- [14]. Herzer. G; "Nanocrystalline soft magnetic alloys", In Handbook of materials", Vol.10ed, Buschow K. H. J, Elsevier pub.co.
- [15]. Schnitzke K., Schultz L., Wecker J. and Katter M.; J. Appl. Phys. Lett., 57, 2853, 1990.
- [16]. Le Chatelier H.; Bull SOC. France Mineral, 10, 204, 1987.

A. K. M. Asaduzzaman, et. al. "Influence of Annealing Condition on Structural Properties of Nano Crystalline Fe_{73.5}Ag₁Nb₃Si_{13.5}B₉Alloy." *IOSR Journal of Applied Physics (IOSR-JAP)*, 12(4), 2020, pp. 14-21.